ELECTROKINETIC AND ELECTROSTATIC PROPERTIES OF BILAYERS CONTAINING GANGLIOSIDES G_{M1}, G_{Dla}, OR G_{T1}.

Comparison with a Nonlinear Theory

ROBERT V. MCDANIEL,* KIM SHARP,‡ DONALD BROOKS,‡§ ALAN C. MCLAUGHLIN,∥ ANTHONY P. WINISKI,¶ DAVID CAFISO,** AND STUART MCLAUGHLIN*
Department of *Physiology and Biophysics, Health Sciences Center, State University of New York, Stony Brook, New York 11794; Departments of ‡Chemistry and §Pathology, University of British Columbia, Vancouver, British Columbia V6T1W5; ∥Department of Biochemistry and Biophysics, University of Pennsylvania, Philadelphia, Pennsylvania 19104; ¶Department of Biochemistry, State University of New York, Stony Brook, New York 11794; Department of **Chemistry, University of Virginia, Charlottesville, Virginia 22901

ABSTRACT We formed vesicles from mixtures of egg phosphatidylcholine (PC) and the gangliosides G_{M1}, G_{Dla}, or G_{T1} to model the electrokinetic properties of biological membranes. The electrophoretic mobilities of the vesicles are similar in NaCl, CsCl, and TMACl solutions, suggesting that monovalent cations do not bind significantly to these gangliosides. If we assume the sialic acid groups on the gangliosides are located some distance from the surface of the vesicle and the sugar moieties exert hydrodynamic drag, we can describe the mobility data in 1, 10, and 100 mM monovalent salt solutions with a combination of the Navier-Stokes and nonlinear Poisson-Boltzmann equations. The values we assume for the thickness of the ganglioside head group and the location of the charge affect the theoretical predictions markedly, but the Stokes radius of each sugar and the location of the hydrodynamic shear plane do not. We obtain a reasonable fit to the mobility data by assuming that all ganglioside head groups project 2.5 nm from the bilayer and all fixed charges are in a plane 1 nm from the bilayer surface. We tested the latter assumption by estimating the surface potentials of PC/ganglioside bilayers using four techniques: we made ^{31}P nuclear magnetic resonance, fluorescence, electron spin resonance, and conductance measurements. The results are qualitatively consistent with our assumption.

INTRODUCTION

Glycoproteins and glycolipids extend several nanometers from the surface of cell membranes, forming a complex layer known as the glycocalyx (1–3). The electrokinetic properties of these cells are often described by combining the Helmholtz-Smoluchowski and Gouy equations (e.g., reference 4). The Helmholtz-Smoluchowski equation relates the electrophoretic mobility of the cell to the zeta potential, which is usually assumed to be equal to the surface potential. The Gouy equation from the theory of the diffuse double layer relates the surface potential to the charge density. In these classical theories any hydrodynamic drag exerted by the glycolipids or glycoproteins in the glycocalyx is ignored and the charges are assumed to be located at the bilayer surface. These two assumptions are clearly incorrect. Several authors recently combined a form of the Navier-Stokes equation that includes a force term due to the hydrodynamic drag exerted by the glycoca-

lyx with either the linear (3, 5, 6) or nonlinear (7) Poisson-Boltzmann equation. They had to assume a specific model for the hydrodynamic and electrostatic properties of the glycocalyx before they could integrate these equations and calculate the velocity of a cell, such as a human erythrocyte, in an electric field. Levine et al. (3) represented the hydrodynamic properties of the glycocalyx by spheres distributed uniformly within a layer ~10 nm thick. They modeled the electrostatic properties by distributing fixed charges uniformly throughout the glycocalyx, placing them at the surface of the bilayer, or locating them at the outer edge of the glycocalyx. Donath and Voigt (8) assumed the potential is uniform within the glycocalyx, which leads to a higher charge density near the outer edge. All of these models describe some of the electrokinetic properties of erythrocytes. The erythrocyte membrane, however, is too complicated to compare critically the predicted and measured mobilities. A simpler model system is required.

In a previous study we formed membranes with an artificial glycocalyx of known composition by mixing the ganglioside G_{M1} with egg phosphatidylcholine (PC). We observed a reasonable agreement between the measured electrophoretic mobilities and the predictions of the linear theory in 0.1 M NaCl solutions, where the potential is small and the linear theory should be valid (9). In this report we extend the theoretical analysis to the nonlinear range (magnitude of potential >25 mV) and describe new measurements on model membranes formed from mixtures of PC and gangliosides G_{M1}, G_{D1a}, or G_{T1}. We measured the electrophoretic mobility of multilamellar PC/ganglioside vesicles in 0.001, 0.01, and 0.1 M NaCl, CsCl, or TMACl solutions. We also measured the adsorption of manganese, 2-(p-toluidinyl) napthalene-6-sulfonate (TNS), and charged spin label probes to sonicated vesicles, as well as the conductance of planar membranes exposed to nonactin or FCCP; we estimated the electrostatic potentials at the surface of the bilayer from these measurements.

The biological roles of the gangliosides G_{M1}, G_{D1a}, and G_{T1} are not yet well defined (10–12). Nevertheless, these gangliosides are clearly important. They are involved in the binding of viruses (13), toxins (14–15), hormones (16–17), lectins (18), and monoclonal antibodies (19) to cell surfaces and the fusion of cells during development (20). They are the major gangliosides of the human brain (21), and play a role in the action of ethanol on membranes (22) and the recovery of brain tissue from electrical lesions (23).

MATERIALS AND METHODS

Materials

Gangliosides G_{M1}, G_{D1a}, and G_{T1} (Supelco, Bellefonte, PA) were analyzed by thin layer chromatography using silica gel G-plates and a solvent system of $CHCl_3$:CH_3OH: 0.02 % (wt/vol) $CaCl_2$ in H_2O (55:45:10; vol/vol). The chromatograms were exposed to iodine vapors or sprayed with either Cu-resorcinol in HCl or 5 % $K_2Cr_2O_7$ in 40 % H_2SO_4. G_{M1} and G_{D1a} ran as major spots ($\approx$ 95 % from densitometric analysis). G_{T1} ran as a major spot with traces of tetrasialo- and disialoganglioside contaminants.

We measured the weight of PC and the weight of ganglioside in each lipid mixture and used the following molecular weights to calculate Q, the uncorrected mole percentage of ganglioside in the mixture: G_{M1}, 1,545; G_{D1a}, 1,836; G_{T1}, 2,127; egg PC, 787; and diphytanoyl PC, 846. We obtained the percentage by weight of sialic acid for each lot of ganglioside from Supelco and calculated the ratio, R, of the measured sialic acid content to the theoretical content. R was 0.95 for G_{M1} and G_{D1a}, and 0.83 for G_{T1}. Supelco (G. Walker, personal communication) claims that the value of $R = 0.83$ probably underestimates the purity of G_{T1}, but our densitometric analysis of G_{T1} agreed qualitatively with this figure. The corrected mole percentage $P = QR$ is plotted on the abscissa in Fig. 2 and is listed in Tables I–IV.

Egg or diphytanoyl PC, bovine brain phosphatidylserine, bovine sphingomyelin, and egg phosphatidylglycerol were obtained from Avanti Biochemicals (Birmingham, AL). Porcine erythrocyte sphingomyelin and standard fatty acid methyl esters for gas-liquid chromatography were purchased from Supelco. Gas-liquid chromatography of ganglioside fatty acid methyl esters was performed with 3% SE-30 on Chromosorb W (Supelco) at 30 ml/min carrier gas flow, with a temperature ramp of 10°/min from 100° to 250°C. Aqueous solutions were prepared with 18

MΩ cm water (Super-Q, Millipore Corp., Bedford, MA) that was subsequently bidistilled in an all-quartz apparatus. They were buffered to pH 7.5 with 0.1–10 mM 4-morpholinepropane sulfonate (Mops) (P-L Biochemicals, Milwaukee, WI). Nonactin was a gift from B. Stearns (Squibb, New Brunswick, NJ). FCCP was purchased from Pierce Chemical Co. (Rockford, IL). Alkali metal chloride salts were obtained from Baker (Phillipsburg, NJ) or Ventron (Danvers, MA). Tetramethylammonium chloride (TMA) was obtained from Aldrich (Milwaukee, WI) and recrystallized before use.

In all our experiments we assume that the gangliosides and egg PC are uniformly mixed in the plane of the membrane. This assumption is probably valid for egg PC/G_{M1} vesicles (24–28). Calorimetric measurements have been made on gangliosides (29) and on vesicles formed from gangliosides and dipalmitoylphosphatidylcholine (28), but we know of no relevant studies on egg PC/G_{D1a} or egg PC/G_{T1} membranes.

Electrophoretic Mobility Measurements

Multilamellar vesicles for microelectrophoresis experiments were prepared according to Bangham et al. (30). Egg PC or defined mixtures of gangliosides and egg PC were vacuum dried in glass round-bottom flasks from chloroform/methanol/water mixtures. The mean value of the electrophoretic mobility was unaffected by the chloroform/methanol/water ratio; the standard deviation was affected by this ratio. We obtained the lowest standard deviations when we co-dissolved PC and G_{M1} in chloroform, PC and G_{D1a} in methanol/water 33:1, or PC and G_{T1} in methanol. All the mobilities we report are the average of two sets of measurements on 10 vesicles in the presence or absence of 10^{-6} M EDTA, which did not significantly affect the results. We measured electrophoretic mobilities at $T = 25°C$ with a Rank Bros. Mark I instrument (Bottisham, Cambridge, U.K.) as described previously (31, 32) and calculated the apparent zeta potential, ζ, from the electrophoretic mobility, μ, using the Helmholtz-Smoluchowski equation:

$$\zeta = \mu \eta / \epsilon_0 \epsilon_r, \tag{1}$$

where ϵ_r is the dielectric constant of the aqueous solution, ϵ_0 is the permittivity of free space, and η is the viscosity of the aqueous solution. By definition, the zeta potential is the electrostatic potential at the hydrodynamic plane of shear (33). For large particles with smooth surfaces it is related to the mobility by Eq. 1. For PC/ganglioside vesicles, however, we emphasize that there is no simple relationship between the zeta potential and electrophoretic mobility. We report the mobilities of these vesicles as apparent zeta potentials, in units of mV calculated from Eq. 1, to facilitate comparison with data in the literature. The average standard deviations of the zeta potentials were 2.8, 1.7, and 0.9 mV for 0.001, 0.01, and 0.1 M salt solutions, respectively.

Alkali metal cations have little effect on the mobility of PC vesicles (32): the zeta potentials of PC vesicles in 0.001, 0.01, and 0.1 M solutions of NaCl and CsCl do not differ significantly from zero. However, PC vesicles have zeta potentials of about -5 mV in 0.001, 0.01, and 0.1 M solutions of TMACl. For each of the monovalent cations, Na, Cs, and TMA, we averaged the zeta potentials of the PC vesicles in the 0.001, 0.01, and 0.1 M salt solutions and plotted these average values at the left hand side of the panels in Fig. 2.

Nuclear Magnetic Resonance Measurements

The effect of manganese on the linewidth of the ^{31}P NMR signal from PC/ganglioside vesicles was described previously (9). Sonicated vesicles were formed by mixing solutions of PC (in chloroform) and ganglioside (in 2:1 chloroform/methanol), evaporating the solvent, adding a buffered NaCl solution, sonicating, centrifuging, and equilibrating the outside of the vesicles with a buffered NaCl solution containing known concentrations of manganese. The 0.1 M NaCl solutions were buffered to pH 7.4 with 5 mM Mops. The 0.01 M solutions were buffered to pH 7.4 with 0.5

mM Mops.[1] The experiments were performed at 25°C. We assumed that the PC/ganglioside ratio is the same on the inner and outer monolayers. This assumption is consistent with EPR studies (34), neuraminidase digestion studies (35), and experiments with a glycolipid exchange protein (T. E. Thompson, personal communication), although no direct measurement of the distribution has been made. We also assumed that the lifetime of the manganese-phosphodiester inner sphere complex is identical for PC vesicles and for PC/ganglioside vesicles. We measured the linewidth of the broadened ^{31}P resonance from the outside monolayer of the vesicles using a radio frequency pulse sequence that nulled the ^{31}P NMR signal from phospholipids in the inner monolayer (9, 36). We plotted the linewidth as a function of external manganese concentration. When this relation is linear, as observed, the slope is proportional to the manganese concentration at the bilayer surface, which is related to the surface potential via the Boltzmann relation.

Fluorescence Measurements

Eisenberg et al. (32) described the use of TNS to probe the electrostatic potential at the hydrocarbon-water interface of phospholipid bilayers. This anionic fluorescent probe (Sigma Chemical Co., St. Louis, MO) was added to sonicated vesicle preparations (37) in aqueous solutions containing 0.01–0.1 M NaCl, 0.1 mM EDTA, 0.5 mM Mops, pH 7.5, $T = 25°C$. The net fluorescence intensity is proportional to the number of TNS molecules adsorbed to the membrane, which is proportional to the concentration of the probe in the aqueous phase immediately adjacent to the membrane. This concentration is related to the electrostatic potential by the Boltzmann relation. We assume that the quantum yield of TNS adsorbed to PC, PC/PG, PC/PS, and PC/ganglioside vesicles is the same because the corrected excitation and emission spectra of TNS adsorbed to these vesicle preparations are nearly identical (data not shown).
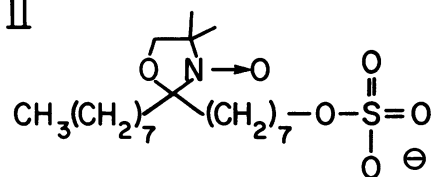
Electron Spin Resonance Measurements

Paramagnetic amphiphiles have been used to estimate the electrostatic potential at the surface of sonicated lipid vesicles (38–41). We used both the alkylammonium (I) and alkylsulfate (II) ester probes illustrated
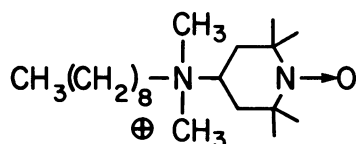
above to determine the surface potentials of sonicated PC/PS and PC/G_{M1} vesicles. The partitioning of the probes between the membrane and the aqueous phase, λ, was determined by calibrating the signal

---

[1] The calculated values of the surface potential for vesicles containing PS were identical at pH 4, 5, and 6 (data not shown). At pH 7.4 the apparent value of the surface potential of a PC/PS vesicle containing 9 mol % PS changes from −19 to −28 mV. This effect is presumably related to the formation of strong complexes between Mn and the serine moiety at alkaline pH values (61, 62).

intensity of the high-field nitroxide resonance in terms of the concentration of free spin label (see method 2 of reference 38). Binding constants for probes I and II to each sample were obtained from plots of λ^{-1} vs. (lipid concentration)$^{-1}$. The surface potentials were determined from the binding constants using the Boltzmann relation (38).

Probes I and II were synthesized as previously described (41). Sonicated vesicles were prepared in 0.1 and 0.01 M buffered solutions as described above for NMR measurements. The total concentration of lipid in the samples was ~15 mg/ml/ exact phospholipid concentrations were determined by phosphate analysis (42).

Conductance Measurements

Planar lipid bilayer membranes were formed from a 1–2 % solution of PC and ganglioside in n-decane (9). Optically black films ($C = 0.4 \times 10^{-6}$ F/cm^2, $G=5 \times 10^{-9}$ S/cm^2, area 0.015 cm^2) were formed in a Teflon chamber (43). We measured the membrane conductance at low applied potential (25 mV) in aqueous solutions containing 0.5×10^{-6} M nonactin or FCCP at 22°C. The solutions also contained 0.001–0.1 M KCl, 10^{-6} M EDTA, and 0.1–5 mM Mops (pH 7.5). This conductance depends on the equilibrium concentration of nonactin-K or FCCP within the membrane (43–45). This concentration depends exponentially on the electrostatic potential within the membrane according to the Boltzmann relation.

GLOSSARY

Abbreviations

FCCP	carbonylcyanide p-trifluoromethoxyphenylhydrazone
G_{D1a}	N-acetylneuraminylgalactosyl-N-acetylgalactosaminyl(N-acetylneuraminyl)galactosylglucosylceramide
G_{D1b}	galactosyl-N-acetylgalactosaminyl(N-acetylneuraminyl-N-acetylneuraminyl)galactosylglucosylceramide
G_{D3}	(N-acetylneuraminyl-N-acetylneuraminyl)galactosylglucosylceramide
GLC	gas-liquid chromatography
G_{M1}	galactosyl-N-acetylgalactosaminyl(N-acetylneuraminyl)galactosylglucosylceramide
G_{M2}	N-acetylgalactosaminyl(N-acetylneuraminyl)galactosylglucosylceramide
G_{M3}	(N-acetylneuraminyl)galactosylglucosylceramide
G_{T1}	(N-acetylneuraminyl)galactosyl-N-acetylgalactosaminyl(N-acetylneuraminyl-N-acetylneuraminyl)galactosylglucosylceramide
Mops	4-morpholinepropane sulfonate
PC	phosphatidylcholine
PG	phosphatidylglycerol
PS	phosphatidylserine
TLC	thin layer chromatography
TNS	2-(p-toluidinyl)napthalene-6-sulfonate.

Mathematical Symbols

β	Head group thickness
γ	Friction parameter, $= (6\pi \, aN)^{1/2}$
ϵ_0	Permittivity of free space
ϵ_r	Dielectric constant of aqueous solution
ζ	Zeta potential
η	Viscosity of aqueous solution
κ	Debye-Hückel parameter
μ	Electrophoretic mobility, $= U/E$
ρ	Volume density of fixed charge
ρ_m	Volume density of mobile charge
σ	Surface charge density

ψ	Electrostatic potential
a	Effective Stokes radius of monosaccharide
C	Capacitance
e	Magnitude of electronic charge
E	Applied electric field
G	Conductance
k	Boltzmann's constant
N	Number density of monosaccharides
T	Absolute temperature
u	Fluid velocity
U	Fluid velocity as $x \rightarrow \infty$
x	Coordinate normal to membrane surface
y	Electrostatic potential in dimensionless units, $= e\psi / kT$.

THEORY

We calculated the electrophoretic mobilities of the vesicles by solving numerically the combination of the Navier-Stokes and nonlinear Poisson- Boltzmann equations (7). Numerical methods allowed us to calculate the mobility for any distribution of charges and monosaccharide elements in the glycocalyx illustrated in Fig. 1.

We first calculated the electrostatic potential normal to the membrane surface, $\psi = \psi(x)$, from the volume density of fixed charge, $\rho = \rho(x)$, using the one dimensional nonlinear Poisson-Boltzmann equation

$$\frac{d^2y}{dx^2} - \kappa^2 \sinh (y) = \frac{-\rho e}{\epsilon_0 \epsilon_r kT},\qquad(2)$$

where $y = e\psi / kT$ for a 1:1 electrolyte, e is the magnitude of the electronic charge, T is the absolute temperature, k is the Boltzmann constant, and $1/\kappa$ is the Debye length. The two boundary conditions are:

$$y \rightarrow 0 \text{ as } x \rightarrow \infty$$

and

$$\frac{dy}{dx} = \frac{-\sigma e}{kT\epsilon_0 \epsilon_r}\qquad(3)$$

at the lipid bilayer surface ($x = -\beta$, see Fig. 1), where σ is the fixed surface charge density (charge/area) in that plane. The fixed charges on monovalent G_{M1}, divalent G_{D1a}, and trivalent G_{T1} were assumed to be (a) located in a plane[2] at a position x within the glycocalyx ($-\beta < x < 0$), (b) uniformly distributed within the glycocalyx, or (c) distributed so as to produce a uniform potential within the glycocalyx.[3] We then calculated the electrophoretic mobil-

---

[2]A plane of charge density σ' (charge/area) at a position x could be represented by a distribution with a Gaussian shape centered at x, or as a difference in the gradient of the potential equal to $-\sigma' e/kT\epsilon_r\epsilon_0$ (Eq. 3). If the width of the Gaussian is <0.3 nm the two representations give the same results within the accuracy of our computer program.

[3]Donath and Voigt (personal communication) found an elegant analytical expression, valid for arbitrarily large potentials, for the electrophoretic mobility when the potential is constant throughout the glycocalyx (i.e., the interfacial electrostatic free energy is a minimum).
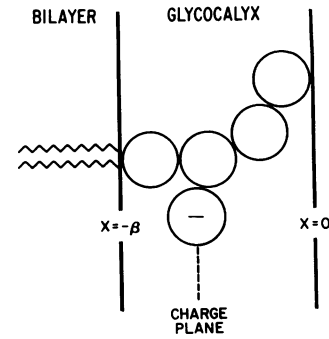

FIGURE 1 Diagram of the glycocalyx of a PC/G_{M1} membrane. For hydrodynamic calculations we consider each monosaccharide a sphere of radius a and assume the spheres are distributed uniformly throughout the glycocalyx, which extends from $x = -\beta$, the surface of the bilayer, to $x = 0$. For electrostatic calculations we ignore the volume of the monosaccharides. We assume the fixed charges on the ganglioside are smeared uniformly over a y-z plane located at x ($-\beta < x < 0$). We make all the conventional assumptions implicit in the Gouy-Chapman theory of the diffuse double layer. Specifically, we assume that the dielectric constant is equal to its bulk aqueous value for $x > -\beta$ and that ions are point charges. We ignore image charge effects and assume mobile ions can penetrate the glycocalyx but are excluded from the bilayer ($x < -\beta$).

ity by considering the membrane to be fixed and calculating the electro-osmotic fluid velocity, u, from the one dimensional Navier-Stokes equation

$$\frac{d^2u}{dx^2} - \gamma^2 u + \rho_m E/\eta = 0,\qquad(4)$$

where $u = u(x)$ is the fluid velocity parallel to the surface, E is the applied electric field, and $\rho_m = \rho_m(x)$ is the charge density (charge/volume) due to the mobile ions, which is calculated from the potential using

$$\rho_m = (\kappa^2 \epsilon_0 \epsilon_r kT/e) \sinh (y)\qquad(5)$$

The friction parameter, $\gamma^2 = 6\pi Na$, is calculated from the effective Stokes radius of the sugar moieties, a, and the number density of monosaccharides $N = N(x)$ (monosaccharides/volume). The densities of both the fixed charges and monosaccharides are zero for $x > 0$. Eq. 4 is subject to the boundary conditions that $u = 0$ at the hydrodynamic plane of shear and that $u \rightarrow -U$ as $x \rightarrow \infty$, where U/E is the electrophoretic mobility.

As well as varying the distribution of fixed charges within the glycocalyx, we varied the radius of each monosaccharide, a, between 0 and 0.8 nm; the thickness of the head group layer, β, between 1.0 and 3.5 nm; and the location of the hydrodynamic plane of shear between $-\beta$ and 0.4β. The number density of monosaccharides was calculated from the mole percentage of gangliosides in the vesicle, assuming a molecular area within the bilayer of 0.7 nm^2 for both the phospholipids and gangliosides. There are 5, 6, and 7 monosaccharides per molecule of G_{M1}, G_{D1a}, and G_{T1}, respectively. We assumed that the monosaccharides are uniformly distributed within the glycocalyx ($N(x)$

is constant for $-\beta < x < 0$) to calculate the viscous drag they exert.

RESULTS

Fig. 2 illustrates that the electrophoretic mobility of multi-lamellar PC/ganglioside vesicles becomes more negative as either the mol percentage of ganglioside in the bilayer increases or the ionic strength decreases. The left-hand scale expresses the mobility in units of velocity/applied electric field and the right-hand scale quantifies the mobility in terms of the apparent zeta potential, calculated from Eq. 1. We measured the electrophoretic mobility of vesicles in NaCl, CsCl, and TMACl solutions. PC vesicles have zero mobility in NaCl or CsCl solutions, indicated by the points at the left in Fig. 2. PC vesicles are slightly negative
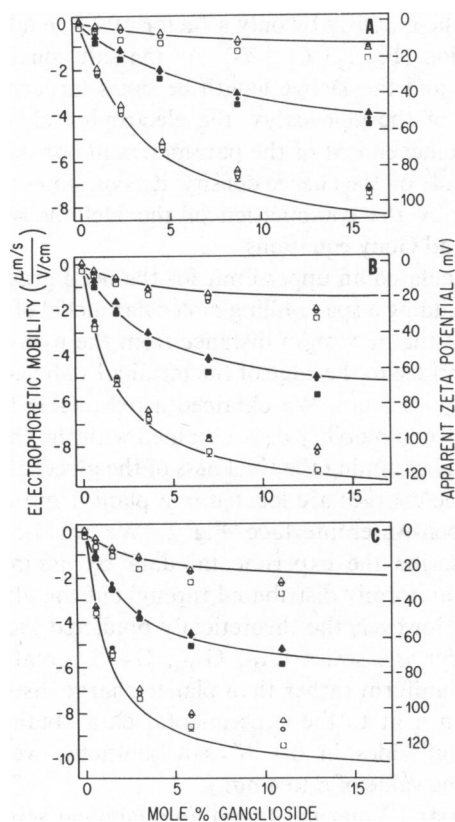
in TMACl solutions for reasons we do not understand. Addition of gangliosides to PC does not alter the magnitude of this small (~5 mV) negative shift. With the exception of this effect of TMA, the electrophoretic mobilities of PC/ganglioside vesicles are similar in Na, Cs, or TMA, suggesting that these ions do not bind significantly to gangliosides (9). On the other hand, the ionic strength strongly affects the mobility: as ionic strength decreases the screening of fixed charges on the vesicles decreases, the electrostatic potential adjacent to the vesicle becomes more negative, and the magnitude of the electrophoretic mobility increases. When the zeta potential is large, it changes ~42 mV for each 10-fold decrease in ionic strength. Similar results were obtained with phospholipid vesicles (see Appendix A of reference 46).

The theory predicts a somewhat stronger dependence of mobility on ionic strength than is observed: when the potential is large the theoretical zeta potential illustrated in Fig. 2 changes by 55–58 mV/ 10-fold change in ionic strength.[4]

It is apparent from Fig. 2 that the relationship between the electrophoretic mobility and the mol percentage ganglioside is approximately linear when the charge density is low, but is nonlinear when the charge density is high. This nonlinearity arises because the electrostatic potential adjacent to the charges becomes more negative as the charge density increases: when the magnitude of this potential is >25 mV, Eq. 2 predicts that the potential does not depend linearly on charge density. This effect leads to a nonlinear dependence of mobility on ganglioside concentration.

The mobility depends on the valence of the ganglioside in the manner predicted by the theory. As the ionic strength and charge density decrease, the mobility should become proportional to the valence of the ganglioside. In 0.001 M salt solutions, where the Debye length is 10 nm, the dimensions of the ganglioside head groups (<3.5 nm) and the other parameters in the model should have little influence on the mobility, which should be determined predominantly by the fixed charge density on the vesicle. The experimentally observed initial slopes with PC/G_{M1}, PC/G_{D1a}, and PC/G_{T1} vesicles are -28, -48, and -71 mV/mol %, respectively in 0.001 M CsCl solutions (see circles in Fig. 2). The theory predicts slopes of -27, -48, and -63 mV/mol %, in reasonable agreement with the results (see curves in Fig. 2). In the nonlinear region the mobility depends less strongly on the valence. For example, at high mole percentage ganglioside the differences between G_{D1a} and G_{T1} are not large (Fig. 2).

FIGURE 2 Electrophoretic mobility of multilamellar vesicles formed from mixtures of egg PC and the gangliosides: (A) G_{M1}, (B) G_{D1a}, (C) G_{T1}. The vesicles were suspended in an aqueous solution of NaCl (triangles), CsCl (circles), or TMACl (squares) buffered to pH 7.5 at 25°C with 0.1–1 mM Mops. In each panel, the upper set of open symbols represents 0.1 M salt solutions, the middle set of filled symbols represents 0.01 M salt solutions, and the lower set of open symbols represents 0.001 M salt solutions. The standard deviations for the TMACl data are illustrated by vertical lines descending from the squares when the standard deviation is greater than the size of the symbol. We calculated the theoretical curves by assuming that no ions bind to the lipids, that the fixed charges on the gangliosides are in a plane 1 nm from the bilayer surface, that the hydrodynamic plane of shear is at the surface, that each monosaccharide in the glycocalyx layer is an independent sphere of Stokes radius 0.35 nm, and that all monosaccharides are uniformly distributed in a 2.5 nm-thick layer.

In summary, the theoretical curves in Fig. 2 provide a qualitative description of the measured mobilities. We calculated these curves by making four assumptions: the monosaccharides in the gangliosides behave as Stokes spheres of radius 0.35 nm, the plane of shear is at the surface of the bilayer, the Stokes spheres are uniformly distributed in a 2.5-nm thick layer, and all the charges are in a plane 1 nm from the surface of the bilayer.

Fig. 3 illustrates the sensitivity of the theoretical curves to these assumptions. In Fig. 3 A we consider the effects of the Stokes radius of the monosaccharide on the predicted mobility. The predictions of the model are similar for radii from 0.2 to 0.8 nm, a range that includes the Stokes radius of glucose (0.35 nm, see reference 47). In Fig. 3 B we vary the distance between the shear plane and the hydrocarbon-water interface. The location of the shear plane is important only if it is outside of the glycocalyx. If it is within the glycocalyx its position has little effect on the electropho-

retic mobility because the profile of fluid velocity is flat throughout most of the glycocalyx (3). However, when all charges are at the vesicle surface and the lipid head groups exert no hydrodynamic drag, the mobility is predicted to depend strongly on the location of the shear plane (46).

Figs. 3 C and 3 D illustrate the effects that the thickness of the glycocalyx and the location of the charge plane have on the predicted mobilities. Decreasing the thickness of the glycocalyx or placing the charge plane further from the surface increases the mobility. These parameters can affect the mobility significantly, even when they vary within a physically reasonable range. For example, decreasing the thickness of the glycocalyx from 2.5 to 1 nm (Fig. 3 C) or increasing the charge plane-bilayer distance from 1 to 2.5 nm (Fig. 3 D) enhances the mobility by a factor of 3 in a 0.1 M salt solution. However, these changes enhance the mobility by only a factor of 1.4 in a 0.001 M salt solution (Figs. 3 C, 3 D). As the salt concentration decreases and the Debye length becomes larger than the thickness of the glycocalyx, the electrophoretic mobility becomes independent of the parameters in our model and depends only on the charge density; it asymptotes the value predicted by the combination of the Helmholtz-Smoluchowski and Gouy equations.

We calculated an upper limit for the head group thickness by building a space-filling molecular model of G_{Tl} and measuring the maximum distance from the hydrocarbon-water interface to the edge of the terminal sialic acid. This distance is ~3.5 nm. We obtained a reasonable fit to the electrophoretic mobility data obtained with the three gangliosides by assuming the thickness of the glycocalyx is 2.5 nm and the charges are located in a plane 1 nm from the hydrocarbon-water interface (Fig. 2). We can also qualitatively describe the experimental data by assuming the charge is uniformly distributed throughout the glycocalyx (Fig. 4). However, the theoretically predicted increase in mobility for the series G_{Ml}, G_{Dla}, G_{Tl} is greater if we assume a uniform rather than planar charge distribution. (To obtain a fit to the experimental data obtained with three gangliosides in 0.1 M salt solutions, we had to increase the value of β to 4 nm.)

Donath and Voigt (8) found an analytical solution for the mobility when the potential is constant throughout the glycocalyx. This constant potential requires some of the charge to be distributed uniformly throughout the glycocalyx and the rest to be concentrated in a plane at the outer edge. The fraction of the total charge at the outer edge must be increased as the ionic strength is decreased. The ratio of charge dispersed throughout the glycocalyx to that at the outer edge is approximately equal to the ratio of the glycocalyx thickness to the Debye length. Thus the equipotential distribution requires a substantial redistribution of charge in response to a change in the ionic strength. Fig. 4 shows that the equipotential distribution predicts higher mobilities than the uniform distribution due to the concentration of charge farther from the membrane surface.
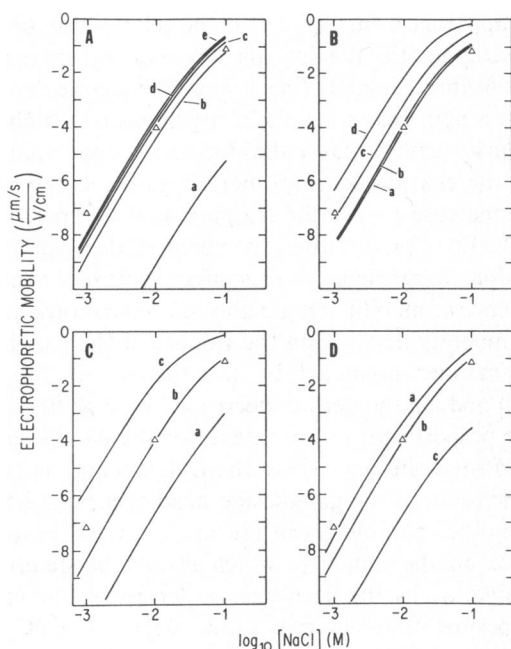

FIGURE 3 (A) Stokes radius of monosaccharides: effect on electrophoretic mobility. We calculated the curves by assuming the thickness of the glycocalyx is 2.5 nm, the fixed charges are located in a plane 1.0 nm from the surface of the bilayer, and the shear plane is at the surface of the bilayer. The Stokes radius, a (in nanometers), of each monosaccharide is 0.0 (a), 0.2 (b), 0.4 (c), 0.6 (d), 0.8 (e). In this figure and in Figs. 3 B, 3 C, and 3 D, the triangles represent experimental data for PC/G_{Ml} vesicles containing 16 mol % G_{Ml} in NaCl solutions (see Fig. 2). (B) Location of shear plane: effect on electrophoretic mobility. The plane of shear is at the bilayer surface (a), in the center of the glycocalyx (b), at the outer edge of the glycocalyx (c) and 1.0 nm beyond the glycocalyx (d). In this panel and in Fig. 3 C and 3 D, we assume that $a = 0.35$ nm and that the other parameters have the values indicated in Fig. 3 A. (C) Thickness of glycocalyx : effect on electrophoretic mobility. The thickness (in nanometers) of the glycocalyx is 1.0 (a), 2.5 (b), 5.0 (c). (D) Location of charge plane: effect on electrophoretic mobility. The charge plane is at the bilayer surface (a), 1.0 nm from the surface (b), and at the outer edge of the glycocalyx (c).
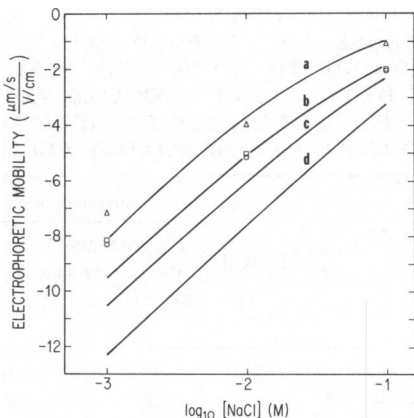
FIGURE 4 Effect of uniform and equipotential charge distributions on electrophoretic mobility. Experimental data for PC vesicles containing 16 mol % G_{MI} (triangles), 13 mol % G_{DIa} (squares), and 11 mol % G_{TI} (circles) in NaCl solutions. We calculated the curves by assuming the monosaccharide radius is 0.35 nm, the thickness of the glycocalyx is 4.0 nm, and the plane of shear is at the surface of the bilayer. For the first three curves we assume the charge is distributed uniformly through the glycocalyx: charge corresponding to 16 mol % G_{MI} (*a*), 13 mol % G_{DIa} (*b*), 11 mol % G_{TI} (*c*). We calculated curve D by assuming the charge corresponding to 11 mol % G_{TI} is distributed to produce a uniform potential within the glycocalyx.

We have considered models in which the fixed charges are located in a plane, distributed uniformly throughout the glycocalyx, or distributed to produce a uniform potential in the glycocalyx. All these models assume the charges are not located at the surface. We tested this assumption by measuring the surface potential of PC/ganglioside bilayers. We compared these potentials with measured surface potentials of PC/PS and PC/PG membranes. We know that the charges on PS and PG are close to the bilayer surface. If, as we assume, the charges on the ganglioside membranes are 1 nm from the surface they should produce a less negative surface potential. The potential at the bilayer surface should be less negative than the potential at the charge plane by a factor of approximately $e^{-\kappa x}$, where $1/\kappa$ is the Debye length and x is the distance from the bilayer surface to the charge plane (24). We used four different techniques to estimate the surface potential. We measured the adsorption of manganese (^{31}P NMR), TNS (fluorescence), spin labels (epr), and ionophores (conductance). The application of three of these techniques to PC/G_{MI} bilayers in 0.1 M salt solutions has been described in detail (9).

We have extended these surface potential measurements to include lower salt concentrations and the gangliosides G_{DIa} and G_{TI}. The results are shown in Tables I–IV. Table I summarizes NMR results obtained with sonicated vesicles formed from mixtures of PC and 1.2–10 mol % negatively charged phospholipid or ganglioside. In 0.1 M salt solutions, the measured potential varies linearly with mole percentage negative lipid. The surface potential changes 2.0 or 2.1 mV/mol % PG or PS, respectively,[1] and

1.1, 1.8, and 3.0 mV/mol % G_{MI}, G_{DIa}, or G_{TI}, respectively. Thus in 0.1 M NaCl the surface potentials of PC/ganglioside vesicles are ~50 % lower than those of PC/PS or PC/PG vesicles of equivalent surface charge, supporting our claim that the charges on the ganglioside are located a significant distance from the surface. Table I illustrates that the surface potentials of the PC/phospholipid and PC/ganglioside vesicles become more negative as the salt concentration decreases, a result that agrees with the predictions of our theory, and most other similar theories. By analyzing this dependence of the surface potential on the Debye length, we obtain support for our postulate that the charges on the gangliosides are located ~1 nm from the surface.[5]

Table II summarizes the fluorescence results. We measured similar surface potentials for the PC/PS and PC/PG vesicles, in agreement with the NMR results. In 0.1 M salt solutions the PC/ganglioside vesicles have ~ one half the surface potential of the PC/PG vesicles even though the PC/G_{DIa} or PC/G_{TI} vesicles have two or three times more fixed charge than the PC/PG vesicles. This result is consistent with our assumption that the charges on gangliosides are ≥ 1 nm from the bilayer surface.[5]

Table III summarizes the electron spin resonance results. The surface potentials of the PC/PS vesicles measured with the alkylammonium probe, I, agree with the predictions of the Gouy equation. A similar agreement was observed when other positively charged paramagnetic probes were used with negatively charged membranes (38, 39). Probe I reports surface potentials that are significantly less negative in PC/G_{MI} vesicles than in PC/PS vesicles, consistent with our hypothesis that the charge on G_{MI} is a significant distance from the surface of the bilayer.[5]

The anionic paramagnetic probe, II, also reports surface potentials in PC/G_{MI} bilayers that are less negative than those in PC/PS membranes. However, the potentials calculated with this probe for the PC/PS membrane are

---

[5]When all fixed charges are at the surface of the membrane and the charge density is low, the Gouy equation predicts that the surface potential is inversely proportional to the square root of the ionic strength. For PC/PS or PC/PG membranes the theory thus predicts that the ratio of the potential in 0.01 M NaCl to the potential in 0.1 M NaCl, r, is 3, in agreement with the experimental observations in Tables I and II. If the fixed charges are in a plane a distance x from the surface of the membrane, r should be greater than three because the surface potential is proportional to exp(-κx). If we assume $x = 1$ nm, $r = 6$. For PC/ganglioside membranes, we observed average values of $r = 4.5$ and 6 from the NMR (Table I) and fluorescence (Table II) measurements. Thus, the dependence of surface potential on ionic strength observed with the NMR and fluorescence measurements is consistent with our assumption that charges on the PC/ganglioside membranes extend a significant distance from the surface. The dependence of surface potential on ionic strength observed with the epr measurements is not consistent with this assumption: however, the surface potentials of PC/G_{MI} membranes are less negative than the surface potentials of PC/PS membranes, which is consistent with this assumption (Table III).

TABLE I

^{31}P NMR STUDIES OF Mn^{+2} ADSORPTION TO BILAYERS: SURFACE POTENTIALS OF SONICATED VESICLES FORMED FROM MIXTURES OF PHOSPHATIDYLCHOLINE AND NEGATIVELY CHARGE LIPIDS

| Negatively charged lipid | mol % | [NaCl] | Surface potential | | |
			Experimental	Theoretical* A	Theoretical* B
		M	*mV*	*mV*	*mV*
Phosphatidylglycerol	5	0.1	−10	−16	−13
	10	0.1	−20	−30	−24
	5	0.01	−32	−44	−43
Phosphatidylserine[1]	5	0.1	−10	−16	−13
	9	0.1	−19	−27	−22
	5	0.01	−26	−44	−43
Ganglioside G_{M1}	3.5	0.1	−4	−4	
	7.1	0.1	−9	−7	
	3.5	0.01	−13	−23	
Ganglioside G_{DIa}	3	0.1	−6	−7	
	8	0.1	−15	−16	
	3	0.01	−28	−35	
Ganglioside G_{T1}	1.2	0.1	−4	−4	
	2.6	0.1	−10	−8	
	1.2	0.01	−20	−23	

*In this table, and in Tables II and III, we assume that the fixed charges on the phospholipids are at the surface of the bilayer and that the fixed charges on the gangliosides are in a plane 1 nm from the surface. In column A, we ignore binding of sodium to the negative phospholipids. In column B, we assume that sodium binds to the negative lipids with an intrinsic association constant of 1 M^{-1} (31, 32).

TABLE II

FLUORESCENCE STUDIES OF TNS ADSORPTION TO BILAYERS: SURFACE POTENTIALS OF SONICATED VESICLES FORMED FROM MIXTURES OF NEGATIVELY CHARGED LIPIDS WITH PHOSPHATIDYLCHOLINE

| Negatively charged lipid | mol % | [NaCl] | Surface potential | | |
			Experimental*	Theoretical‡ A	Theoretical‡ B
		M	*mV*	*mV*	*mV*
Phosphatidylglycerol	7	0.1	−10	−22	−18
		0.01	−25	−57	−54
Phosphatidylserine	7	0.1	−8	−22	−18
		0.01	−23	−57	−54
Ganglioside G_{M1}	7	0.1	−3	−7	
		0.01	−16	−40	
Ganglioside G_{DIa}	7	0.1	−4	−14	
		0.01	−26	−60	
Ganglioside G_{T1}	6	0.1	−6	−18	
		0.01	−33	−67	

*The average standard deviation was 1 mV.
‡See Table I for details.

TABLE III

EPR STUDIES OF CHARGED SPIN PROBE PARTITIONING TO SONICATED VESICLES: SURFACE POTENTIALS OF SONICATED VESICLES FORMED FROM MIXTURES OF NEGATIVELY CHARGED LIPIDS AND PHOSPHATIDYLCHOLINE

| Negatively charged lipid | mol % | [NaCl] | Surface potential | | | |
			Experimental* Cationic probe (I)	Anionic probe (II)	Theoretical‡ A	Theoretical‡ B
		M	*mV*	*mV*	*mV*	*mV*
Phosphatidylserine	8.5	0.1	−22	−4	−26	−21
	16	0.1	−40	−5	−45	−34
	8.5	0.01	−61	−28	−66	−61
	16	0.01	−90	−46	−95	−84
Ganglioside G_{M1}	9	0.1	−21	—	−10	
	17	0.1	−29	—	−17	
	9	0.01	−49	−14	−47	
	17	0.01	−57	−38	−66	

*The average standard deviations for measurements made using probes I and II were 2 and 4 mV, respectively.
‡See Table I for details.

TABLE IV

CONDUCTANCE STUDIES OF BILAYERS USING NONACTIN-K AND FCCP: ELECTROSTATIC POTENTIALS WITHIN PLANAR BILAYERS FORMED FROM MIXTURES OF PHOSPHATIDYLCHOLINE AND A NEGATIVELY CHARGED LIPID IN DECANE

| Negatively charged lipid | mol % | [KCl] | Potential | | |
			Experimental*	Theoretical‡ A	Theoretical‡ B
		M	*mV*	*mV*	*mV*
Phosphatidylserine	9	0.1	−23	−27	−24
	30	0.1	−49	−71	−55
	50	0.1	−68	−95	−69
Ganglioside G_{M1}	17	0.1	−22	−17	
		0.01	−61	−66	
		0.001	−107	−124	
Ganglioside G_{DIa}	16	0.1	−44	−27	
		0.01	−73	−82	
		0.001	−117	−141	
Ganglioside G_{T1}	12	0.1	−15	−29	
		0.01	−65	−85	
		0.001	−110	−144	

*Average of potentials measured by nonactin-K and by FCCP, relative to phosphatidylcholine/decane bilayers. The potentials are the sum of the double layer potential and any difference in dipole potential.[8] The average standard deviation was 4 mV.
‡We assumed that the fixed charges on the phospholipids are at the surface of the bilayer and that the fixed charges on the gangliosides are in a plane 1 nm from the surface. In column A, we ignore binding of potassium to the negative phospholipids. In column B, we assume that potassium binds to the negative phospholipids with an intrinsic association constant of 0.5 M^{-1}.

significantly less negative than predicted by the Gouy equation. We do not understand why the potentials reported by the anionic probes (see Tables II and III) are signficantly less negative than the potentials reported by the cationic probes (see Tables I and III). This result could be due to a discreteness-of-charge effect (48–57). We are investigating this possibility by making measurements on positively charged membranes.

Table IV summarizes conductance measurements on planar bilayers formed from mixtures of decane, negatively charged lipid, and PC. We measured the conductance due to an anionic probe (FCCP) and a cationic probe (nonactin-K). As negatively charged lipid was added to a PC bilayer, the conductance due to FCCP decreased and the conductance due to nonactin-K increased.[6] In each case, the magnitude of the conductance change was about equal for the oppositely charged probes. Thus, a change in the electrostatic potential within the membrane, which is the sum of the diffuse double layer and dipole potentials, was responsible for the change in conductance.[7] Changes in other parameters, such as fluidity or dielectric constant, would change the conductance produced by the anionic and cationic probes in the same direction. Usai et al. (58) measured the adsorption of the anionic probe tetraphenylborate to PC and PC/G_{MI} planar bilayers. They obtained results similar to those shown in Table IV for PC/G_{MI} bilayers in 0.1 M monovalent salt solutions.

In 0.1 M salt solutions, addition of charge to the membrane produces a less negative potential when the charges are on gangliosides than when they are on PS (Table IV). These observations are also consistent with our assumption that the charges on the gangliosides are located a significant distance (>1nm) from the surface.[8]

The electrostatic potential within individual PC/ganglioside bilayers becomes more negative as the monovalent salt concentration decreases. Table IV shows that the

electrostatic potential was 45 mV more negative when the KCl concentration decreased from 0.01 to 0.001 M. We also estimated the dependence of potential on ionic strength by forming planar bilayers in a 0.001 M KCl solution and adding lithium chloride to both sides of the bilayer until the ionic strength was 0.1 M. We measured the nonactin-K or FCCP conductances of PC/ganglioside planar bilayers formed from mixtures of PC with 17, 16, and 12 mol % G_{MI}, G_{D10a}, and G_{TI}, respectively. The slopes of the potential vs. $\log_{10}$ (ionic strength) curves were 47, 44, and 51 mV/decade for gangliosides G_{MI}, G_{DIa}, and G_{TI}, respectively. Similar results were obtained with charged phospholipids (44–46). All these results agree reasonably well with the predictions of diffuse double layer theory. The Poisson-Boltzmann equation (Eq. 2) predicts that the surface potential should change by ~58 mV/decade ionic strength when the potential is high.

DISCUSSION

We compared our measurements of the electrophoretic mobility of model membranes with the predictions of a theory that uses the nonlinear form of the Poisson-Boltzmann equation. Our main conclusion is that the theory can describe the measurements (Fig. 2) if we make reasonable assumptions about the structure of ganglioside head groups and their hydrodynamic behavior (Fig. 1). The two most important parameters in the theory are the thickness of the glycocalyx and the charge distribution within this layer (Fig. 3). We can account for the electrophoretic mobility data in Fig. 2 if we assume the thickness of the glycocalyx is 2.5 nm, an assumption consistent with the available x-ray diffraction data,[9] and the charges are 1 nm from the surface of the bilayer. We tested the latter assumption by measuring the surface potentials of PC/ganglioside bilayers and comparing them with the surface potentials of phospholipid bilayers, where the charge is at the surface of the bilayer. These measurements did not

---

[6]We also studied the FCCP and nonactin-K conductance of planar bilayers formed from mixtures of the neutral lipid glycerol monooleate (GMO) and G_{MI}. G_{MI} produced a more negative potential within the GMO than within the PC membrane, for reasons that we do not understand. Our results with GMO$_{MI}$ bilayers agree with those of Tosteson et al. (63).

[7]This result disagrees with the suggestion of Usai et al. (58) that incorporation of G_{MI} into a PC bilayer decreases the fluidity of the membrane. They observed that incorporation of G_{MI} increased the time constant for the movement of tetraphenylborate between the two free energy wells at the membrane-solution interfaces, and we confirmed their experimental observation. However, the fluidity of the membrane is not the only factor that affects the time constant. For example, if the ganglioside decreased the concentration of tetraphenylborate in the center of the membrane more than it decreased the concentration in the interfacial wells, the time constant would increase. This could occur because of a discreteness-of-charge effect, as discussed in detail by Andersen et al. (64).

[8]It is possible that the addition of gangliosides to a PC bilayer changes the dipole potential within the membrane. We converted G_{DIa} and G_{TI} to G_{MI} by neuraminidase digestion (35). Since the head groups are identical

to native G_{MI}, the double layer potentials should be identical, but the dipole potentials could be different. We found that G_{MI} formed from G_{DIa} had the same effect on nonactin-K and FCCP conductance of a PC bilayer as native G_{MI}. However, G_{MI} derived from G_{TI} produced a less negative potential (by ~15 mV for 17 mol % G_{MI}) than native G_{MI}, which could explain why G_{TI} produced a less negative electrostatic potential than the other two gangliosides (see Table IV). The unusual dipole potential within PC bilayers containing G_{TI} could be due to the hydroxy-fatty acid content (13 % by weight by GLC) of our sample of G_{TI}. Significant amounts of hydroxy-fatty acids do not occur in G_{MI} or G_{DIa} although they do occur naturally in cerebrosides and in other gangliosides (65–68).

[9]Our assumption that the glycocalyx is 2.5 nm-thick is qualitatively consistent with the 2 nm glycocalyx thickness of PC/G_{MI} bilayers determined from x-ray diffraction (59). X-ray diffraction measurements have been made on hexagonal phases of mixed gangliosides (60), but we know of no diffraction studies of PC/G_{DIa} or PC/G_{TI} bilayers. Our assumption that all gangliosides extend 2.5 nm from the surface of the bilayer is probably an oversimplification.

---

allow us to determine unambiguously the charge distribution, but the four methods we used gave the same qualitative result: the fixed charges on gangliosides have less influence on the surface potential than the fixed charges on phospholipids, presumably because the sialic acid residues are a significant distance from the bilayer surface. This conclusion agrees with x-ray diffraction measurements on PC/G_{M1} bilayers (59).

We further tested the ability of the theoretical model to fit experimental data by measuring the electrophoretic mobility of vesicles formed from mixtures of PC and either G_{M2} or G_{M3}. These gangliosides lack the terminal (G_{M2}) and terminal plus penultimate (G_{M3}) neutral monosaccharides of G_{M1}. These molecules should exert less hydrodynamic drag than G_{M1} and the PC/ganglioside vesicles should move faster in the order $G_{M1} < G_{M2} < G_{M3}$. The proportional increase in mobility should be largest in 0.1 M NaCl, where the Debye length is shortest. The mobilities changed less than we expected.[10] Furthermore, the electrophoretic mobilities of egg PC vesicles containing 15 mol % G_{D1a}, G_{D1b}, or G_{D3} were identical in 0.1 M NaCl although G_{D3} has two fewer neutral sugars than G_{D1a} or G_{D1b}. A more sophisticated hydrodynamic treatment of bilayers containing gangliosides might account for these results.[11]

In conclusion, a simple theoretical model can describe qualitatively the electrophoretic mobility measurements illustrated in Fig. 2. Our model, and other very similar models (5, 6, 8), are superior to the combination of the Helmholtz-Smoluchowski and Gouy equations, which predicts mobilities that are twofold higher than observed experimentally for PC/ganglioside vesicles (9) and human erythrocytes (3) in decimolar salt solutions.

---

[10]If we assume that β, the thickness of the glycocalyx, decreases in proportion to the number of monosaccharide residues per molecule and that N, the number density of monosaccharides, remains constant the theoretically predicted mobilities of PC vesicles containing 17 mol % G_{M1}, G_{M2}, or G_{M3} increase in the ratio 1:1.6:2.6 in 0.1 M salt. The experimentally measured mobilities change much less than predicted: they increase in the ratio of 1 : 1.3 : 1.3 in 0.1 M NaCl (data not shown). (In 0.01 and 0.001 M NaCl solutions the mobilities of PC/G_{M2} and PC/G_{M3} vesicles did not differ significantly from the values obtained with PC/G_{M1} vesicles illustrated in Fig. 2 A). On the other hand, if we assume that β remains constant and N changes in the series G_{M1}, G_{M2}, G_{M3}, the theoretical model predicts only small increases in the electrophoretic mobility of PC/ganglioside vesicles as G_{M1} is replaced by G_{M2} or G_{M3}. This theoretical prediction agrees with the experimental results.

[11]The present theory treats the sugar units in the glycocalyx as noninteracting spheres. Hence, the friction coefficient of a head group is assumed to be directly proportional to the number of sugars units present. If hydrodynamic interactions between the individual sugars within an oligosaccharide head group are taken into account, however, the friction coefficient depends considerably less strongly on the number of monosaccharides per glycolipid. For instance, applying the Kirkwood-Riseman treatment (69) to oligomers containing three to seven units shows that removal of a single monomer reduces the friction coefficient by at most 25– 30% of the reduction calculated if the monomers were noninteracting spheres (70–71).

REFERENCES

1. Parsegian, V. A. 1974. Possible modulation of reactions on the cell surface by changes in electrostatic potential that accompany cell contact. *Ann. N.Y. Acad. Sci.* 238:362–370.

2. Heinrich, R., M. Gaestel, and R. Glaser. 1982. The electric potential profile across the erythrocyte membrane. *J. Theor. Biol.* 96:211–231.

3. Levine, S., M. Levine, K. A. Sharp, and D. E. Brooks. 1983. Theory of the electrokinetic behavior of human erythrocytes. *Biophys. J.* 42:137–145.

4. Aveyard R., and D. A. Haydon. 1973. Introduction to the Principles of Surface Chemistry. Cambridge University Press, Cambridge. 40–57.

5. Donath, E., and V. Pastushenko. 1979. Electrophoretical study of cell surface properties. The influence of the surface coat on the electric potential distribution and on general electrokinetic properties of animal cells. *J. Electroanal. Chem.* 104:543–554.

6. Wunderlich, R. W. 1982. The effects of surface structure on the electrophoretic mobilities of large particles. *J. Colloid Interface Sci.* 88:385–397.

7. Sharp, K. E., and D. E. Brooks. 1985. Calculation of the electrophoretic mobility of a particle bearing bound polyelectrolyte using the nonlinear Poisson-Boltzmann equation. *Biophys. J.* 47:563–566.

8. Donath, E., and A. Voigt. 1983. Charge distribution within cell surface coats of single and interacting surfaces— a minimum free electrostatic energy approach. Conclusions for electrophoretic mobility measurements. *J. Theor. Biol.* 101:569–584.

9. McDaniel, R. V., A. McLaughlin, A. P. Winiski, M. Eisenberg, and S. McLaughlin. 1984. Bilayer membranes containing the ganglioside G_{M1}: models for electrostatic potentials adjacent to biological membranes. *Biochemistry.* 23:4618–4623.

10. Fishman, P. H., and R. O. Brady. 1976. Biosynthesis and function of gangliosides. *Science (Wash. DC).* 194:906–915.

11. Hakomori, S. 1981. Glycosphingolipids in cellular interaction, differentiation, and oncogenesis. *Annu. Rev. Biochem.* 50:733–764.

12. Tillack, T. W., M. Wong, M. Allietta, and T. E. Thompson. 1982. Organization of the glycosphingolipid asialo-G_{M1} in phosphatidylcholine bilayers. *Biochim. Biophys. Acta.* 691:261–273.

13. Tsao, Y. and L. Huang. 1985. Sendai virus induced leakage of liposomes containing gangliosides. *Biochemistry.* 24:1092–1097.

14. Fishman, P. H. 1982. Role of membrane gangliosides in the binding and action of bacterial toxins. *J. Membr. Biol.* 69:85–97.

15. van Heyningen, W. E., and J. E. Seal. 1983. Cholera. The American Scientific Experience, 1947–1980. Westview Press, Boulder, Colorado. 257–266.

16. Poss, A., M. Deleers, and J. M. Ruysschaert. 1978. Evidence for a specific interaction between G_{T1} ganglioside incorporated into bilayer membranes and thyrotropin. *FEBS (Fed. Eur. Biochem. Soc.) Lett.* 86:160–162.

17. Bremer, E. G., S. Hakomori, D. F. Bowen-Pope, E. Raines, and R. Ross. 1984. Ganglioside-mediated modulation of cell growth, growth factor binding, and receptor phosphorylation. *J. Biol. Chem.* 259:6818–6825.

18. Peters, M. W., I. E. Mehlhorn, K. R. Barber, and C. W. M. Grant. 1984. Evidence of a distribution difference between two gangliosides in bilayer membranes. *Biochim. Biophys. Acta.* 778:419–428.

19. Cheresh, D. A., R. A. Reisfeld, and A. P. Varki. 1984. O-acetylation of disialoganglioside G_{D3} by human melanoma cells creates a unique antigenic determinant. *Science (Wash. DC).* 225:844–846.

20. Whatley, R., S. Ng, J. Rogers, W. C. McMurray, and B. D. Sanwal. 1976. Developmental changes in gangliosides during myogenesis of a rat myoblast cell line and its drug resistant variants. *Biochem. Biophys. Res. Commun.* 70:180–185.

21. Svennerholm, L. 1963. Chromatographic separation of human brain gangliosides. *J. Neurochem.* 10:613–623.

22. Harris, R. A., G. I. Groh, D. M. Baxter, and R. J. Hitzemann. 1984. Gangliosides enhance the membrane actions of ethanol and pentobarbital. *Mol. Pharmacol.* 25:410–417.

23. Sabel, B. A., M. D. Slavin, and D. G. Stein. 1984. G_{M1} ganglioside treatment facilitates behavioral recovery from bilateral brain damage. *Science (Wash. DC).* 225:340–341.

24. Hill, M.W., and G. Lester. 1972. Mixtures of gangliosides and phosphatidylcholine in aqueous dispersions. *Biochim. Biophys. Acta.* 282:18–33.

25. Bach, D., I. R. Miller, and B. Sela. 1982. Calorimetric studies on various gangliosides and ganglioside-lipid interactions. *Biochim. Biophys. Acta.* 686:233–239.

26. Sela, B. and D. Bach. 1984. Calorimetric studies on the interaction of gangliosides with phospholipids and myelin basic protein. *Biochim. Biophys. Acta.* 771:177–182.

27. Thompson, T. E., M. Allietta, R. E. Brown, M. L. Johnson, and T. W. Tillack. 1985. Organization of ganglioside G_{M1} in phosphatidylcholine bilayers. *Biochim. Biophys. Acta.* 817:229–237.

28. Myers, M., C. Wortman, and E. Friere. 1984. Modulation of neuraminidase activity by the physical state of phospholipid bilayers containing gangliosides G_{D1a} and G_{T1b}. *Biochemistry.* 23:1442–1448.

29. Maggio, B., T. Ariga, J. M. Sturtevant, and R. K. Yu. 1985. Thermotropic behavior of glycosphingolipids in aqueous dispersions. *Biochemistry.* 24:1084–1092.

30. Bangham, A.D., M. W. Hill, and W. Mille. 1974. Preparation and use of liposomes as models of biological membranes. *Methods Membr. Biol.* 1:1–68.

31. McLaughlin, S., N. Mulrine, T. Gresalfi, G. Vaio, and A. C. McLaughlin. 1981. Adsorption of divalent cations to bilayer membranes containing phosphatidylserine. *J. Gen. Physiol.* 77:445–473.

32. Eisenberg, M., T. Gresalfi, T. Riccio, and S. McLaughlin. 1979. Adsorption of monovalent cations to bilayer membranes containing negative phospholipids. *Biochemistry.* 18:5213–5223.

33. Verwey, E. J. W., and J. Th. Overbeek. 1948. Theory of the Stability of Lyophobic Colloids. Elsevier Science Publishing Co., Inc., New York. 48.

34. Sharom, F.J, and C. W. M. Grant. 1978. A model for ganglioside behavior in cell membranes. *Biochim. Biophys. Acta.* 507:280–293.

35. Felgner, P.L., E. Friere, Y. Barenholz, and T. E. Thompson. 1982. Kinetics of transfer of gangliosides from their micelles to dipalmitoylphosphatidylcholine vesicles. *Biochemistry.* 20:2168–2172.

36. Lau, A., A. C. McLaughlin, and S. McLaughlin. 1981. The adsorption of divalent cations to phosphatidylglycerol bilayer membranes. *Biochim. Biophys. Acta.* 645:279–292.

37. Barenholz, Y., D. Gibbes, B. J. Littman, J. Goll, T. E. Thompson, and F. D. Carlson. 1977. A simple method for the preparation of homogeneous phospholipid vesicles. *Biochemistry.* 16:2806–2810.

38. Castle, J. D. and W. L. Hubbell. 1976. Estimation of membrane surface potential and charge density from the phase equilibrium of a paramagnetic amphiphile. *Biochemistry.* 15:4818–4831.

39. Gaffney, B. J. and R. J. Mich. 1976. A new measurement of surface charge in model and biological lipid membranes. *J. Am. Chem. Soc.* 98:3044–3045.

40. Cafiso, D. S. and W. L. Hubbell. 1981. EPR determination of membrane potentials. *Annu. Rev. Biophys. Bioeng.* 10:217–244.

41. Cafiso, D. S. and W. L. Hubbell. 1980. Light-induced interfacial potentials in photoreceptor membranes. *Biophys. J.* 30:243–264.

42. Bartlett, G. R. 1959. Phosphorous assay in column chromatography. *J. Biol. Chem.* 234:466–468.

43. McLaughlin, S., G. Szabo, and G. Eisenman. 1971. Divalent cations and the surface potential of charged phospholipid membranes. *J. Gen. Physiol.* 58:667–687.

44. McLaughlin, S., G. Szabo, G. Eisenman, and S. M. Ciani. 1970. Surface charge and the conductance of phospholipid membranes. *Proc. Natl. Acad. Sci. USA.* 67:1268–1275.

45. McLaughlin, S. 1977. Electrostatic potentials at membrane solution interfaces. *Curr. Top. Membr. Transp.* 9:71–144.

46. McLaughlin, A., W. -K. Eng, G. Vaio, T. Wilson, and S. McLaughlin. 1983. Dimethonium, a divalent cation that exerts only a screening effect on the electrostatic potential adjacent to negatively charged phospholipid bilayer membranes. *J. Membr. Biol.* 76:183–193.

47. Weast, R. C. 1974. Handbook of Chemistry and Physics. 55th ed. Chemical Rubber Press, Cleveland, Ohio. pp. D31, D205, F60.

48. Grahame, D. C. 1958. Discreteness-of-charge effects in the inner region of the electrical double layer. *Z. Elektrochem.* 62:264–274.

49. Barlow, C. A., Jr., and J. R. MacDonald. 1967. Theory of discreteness of charge effects in the electrolyte compact double layer. *Advan. Electrochem. Electrochem. Eng.* 6:1–200.

50. Levine, S., J. Mingins, and G. M. Bell. 1965. The diffuse layer correction to the discrete ion effect in electric double layer theory. *Can. J. Chem.* 43:2834–2866.

51. Levine, S., J. Mingins, and G. M. Bell. 1967. The discrete ion effect in ionic double layer theory. *J. Electroanal. Chem.* 13:280–329.

52. Levine, S. 1971. Adsorption isotherms in the electric double layer and the discreteness-of-charge effect. *J. Colloid Interface Sci.* 37:619–634.

53. Levine, S., and W. R. Fawcett. 1979. Some aspects of discreteness of charge and ion-size effects for ions adsorbed at charged metal/aqueous electrolyte interfaces. *J. Electroanal. Chem.* 99:265–281.

54. Tsien, R. Y. 1978. A virial expansion for discrete charges buried in a membrane. *Biophys. J.* 24:561–567.

55. Wang, C. -C., and L. J. Bruner. 1978. Evidence for a discrete charge effect within lipid bilayer membranes. *Biophys. J.* 24:749–764.

56. Nelson, A. P., and D. A. McQuarrie. 1975. The effect of discrete charges on the electrical properties of a membrane. *J. Theor. Biol.* 55:13–27.

57. Cole, K. S. 1969. Zeta potential and discrete vs. uniform surface charge. *Biophys. J.* 9:465–469.

58. Usai, C., M. Robello, F. Gambale, and C. Marchetti. 1984. Effect of gangliosides on phospholipid bilayers: a study with the lipophilic ions relaxation method. *J. Membr. Biol.* 82:15–23.

59. McDaniel, R. V. and T. J. McIntosh. 1986. X-ray diffraction studies of the cholera toxin receptor, G_{M1}. *Biophys. J.* 49:93–96.

60. Curatolo, W., D. M. Small, and G. G. Shipley. 1977. Phase behavior and structural characteristics of hydrated bovine brain gangliosides. *Biochim. Biophys. Acta.* 468:11–20.

61. Puskin, J. S. 1977. Divalent cation binding to phospholipids: an EPR study. *J. Membr. Biol.* 35:39–55.

62. McLaughlin, A. C. 1982. Phosphorous-31 and Carbon-13 nuclear magnetic resonance studies of divalent cation binding to phosphatidylserine membranes: use of cobalt as a paramagnetic probe. *Biochemistry.* 21:4879–4885.

63. Tosteson, M. T., D. C. Tosteson, and J. Rubnitz. 1980. Cholera toxin interactions with lipid bilayers. *Acta Physiol. Scand. Suppl.* 21–25.

64. Andersen, O. S., S. Feldberg, H. Nakadomari, S. Levy, and S. McLaughlin. 1978. Electrostatic interactions among hydrophobic ions in lipid bilayer membranes. *Biophys. J.* 21:35–70.

65. Klenk, E., and L. Georgias. 1967. Über zwei weitere Komponenten des Gemischs der Gehirnganglioside. *Hoppe-Seylers Z. Physiol. Chem.* 348:1261–1267.

66. Ghidoni, R., S. Sonnino, M. Masserini, P. Orlando, and G. Tetta-manti. 1981. Specific tritium labeling of gangliosides at the 3-position of sphingosines. *J. Lipid Res.* 22:1286–1295.

67. Siddiqui, B., and R. H. McLuer. 1968. Lipid components of sialosyl-galactosylceramide of human brain. *J. Lipid Res.* 9:366–370.

68. Ledeen, R. W., R. K. Yu, and L. F. Eng. 1973. Gangliosides of human myelin: sialosylgalactosylceramide as a major component. *J. Neurochem.* 21:829–839.

69. Kirkwood, J. G. and J. Riseman. 1948. The intrinsic viscosities and diffusion constants of flexible macromolecules in solution. *J. Chem. Phys.* 16:565–573.

70. Bloomfield, V., W. O. Dalton, and K. E. van Holde. 1967. Frictional coefficients of multisubunit structures. I. Theory. *Biopolymers.* 5:135–148.

71. Cantor, C. R. and P. R. Schimmel. 1980. Biophysical Chemistry II: Techniques for the Study of Biological Structure and Function. W. H. Freeman and Co., San Francisco. 565–570.